

DOI: [http://dx.doi.org/10.21123/bsj.2020.17.2\(SD\).0642](http://dx.doi.org/10.21123/bsj.2020.17.2(SD).0642)

Studying the Effect of Magnesium Oxide Nanoparticles Prepared on the Surface of Poly Methyl Methacrylate

Mustafa F. Al-Rawi¹

Ahmed Mishaal Mohammed^{2*}

Hameed K. AL-Duliami¹

Received 21/9/2019, Accepted 26/1/2020, Published 23/6/2020



This work is licensed under a [Creative Commons Attribution 4.0 International License](https://creativecommons.org/licenses/by/4.0/).

Abstract:

In this paper, magnesium oxide nanoparticles (MgO NPS) have been prepared and characterized and its concentration effect has been studied on polymers surface (MgO NPS). The results showed that the degradation of poly methyl methacrylate increased when using such metal oxide. The results also showed that the metal oxide increased the degradation of poly methyl methacrylate. X-ray diffraction, scanning electron microscopy, atomic force microscopy were used to study the morphological characteristics and size of nano MgO particles analysis. Films were prepared by mixing the different masses of MgO NPS (0.025, 0.05, 0.1, 0.2 and 0.4) % with a polymer solution ratio (W/V) 7 %. Photo- degradation rate was monitored irradiation's time by measuring the incident frequency of the index value of the hydroxyl coefficient of growth (I_{OH}) at fixed film thickness and constant concentration. Spectrophotometry (IR, and UV. Visible) techniques were used to determine the change in the intensity of the spectrum bundles.

Key words: Magnesium oxide, Photo-degradation, Poly methyl methacrylate, MgO NPS, Nanoparticles.

Introduction:

Nanoparticles are engineered materials at the molecular/atomic construction (1-100) nm altogether unique in relation to their bulk counterparts (1). Polymers are considered to be an excellent host material for nanoparticles of metals (2, 3). The addition of inorganic compounds such as Zn, Mg, Ni, or element oxide like CuO, MgO can enhance the electrical properties of these polymers (4), an inorganic fillers are incorporated into a poly methyl methacrylate to show appear composites with enhanced automatic, thermic, and roadblock properties compared to the polymer matrix (5). The photolysis of PMMA which is result from a haphazard scission of the polymer constraint backbone caused by a radical react. Three essential reactions (Unorganized hemolytic scission of main-chain (C = C) bonds, photo-dissociation of the methyl side-groups and photolysis of the ester side-groups) are reported be done at the same time. Monomer formative through radiation to chain depolymerization after photolytic cleavage of main chains (6). When PMMA is blending with inorganic materials like ZrO_2 , SiO_2 or TiO_2 at the nanometer level, the product obtained that hybrid materials has

high strength and thermal stability (7). The strength of reacting ultra-violet (UV) photons (e.g. UVA, UVB, UVC etc.) with the polymer chains are indeed a concern. The degradation of PMMA has been studied in a wide range of UV-wavelengths (248, 193 and 157) nm (8) at different exposure times. Generally, all the polymers study show a pronounce degradation with increasing irradiation time successive to high numbers of chain cleavage (9). The degradation of polymer, formed shorter chains, that initiated by the chain scission process due to the photo-excitation of atoms that bear an unpaired electron or double bond (10). Mixed metal oxides have fascinating optical, electrical, magnetic, adsorbent, catalytic and chemical properties, which are not typically observed in the single individual components (11, 12). MgO nanostructures are synthesized by dehydration of $Mg(OH)_2$ or by decomposition of various magnesium precursors using sol-gel (13), thermal evaporation (14), surfactant methods (15), chemical vapor deposition (16), flame spray pyrolysis (17), and hydrothermal. However, PMMA, due to its photochemical properties, is not suitable for durable application in outdoor condition (18, 19). In this study, a new type of MgO NPS was prepared by using precipitation method and used as a UV photo inducer for PMMA degradation.

¹Department of Chemistry, College of Education for Pure Sciences, University of Anbar, Ramadi, Iraq.

²Department of Chemistry, College of Science, University of Anbar, Ramadi, Iraq.

* Corresponding author: sc.dr.ahmedm.mohammed@uoanber.edu.iq

* ORCID ID: <https://orcid.org/0000-0002-1426-5929>

Materials and Methods:

All materials used in the preparation method were bought from British drug houses (BDH) and the deionized distilled water was used throughout the work, so the analytical grade of this study was based on all of the chemicals and reagents.

Preparation of magnesium oxide

7.42 g of magnesium nitrate was dissolved in 50 mL distilled water, inside a 500 mL volumetric flask and 10 g of sodium hydroxide was dissolved in 250 mL of deionized water, both were constantly stirred by magnetic stirrer for 45 mins. Sodium hydroxide solution was added to magnesium nitrate solution gradually (drop by drop) using burette at room temperature (20,21). After half an hour, a white deposit was observed, after filtration by using (Gravity filtration) and drying of the solution, the output was burned inside a preheated oven maintained at 400 °C for 3 hours to obtain the nanoparticles.

Preparation of PMMA solution

7 g of methyl methacrylate polymer desolves in volume 100 mL of chloroform (7% W/V) with continuous blending using magnetic stirrer at room temperature to ensure homogenization for one hour.

Preparation of polymeric films

In the chloroform solvent, 1 mL of solvent soluble magnesium oxide was mixed in 3 mL PMMA solution with different weight ratios (0.025, 0.05, 0.1, 0.2, and 0.4) % (22). Then the volumes taken from the above steps were combined well to ensure high homogeneity and make sure there are no bubbles. The mixture was then poured into 4 mL glass molds made of glass slides mounted on a piece of glass placed on a horizontal surface that was adjusted with the settlement balance to ensure that the solution was evenly distributed in the mold. Then, the mixture is left for 24 hours at room temperature to dry and then remove it with a blade taking into consideration that the thickness of the film was about 70 ± 5 micrometers using the micrometer. The films were then cut into dimensions 1.5-3.5 cm in accordance with the spectral devices (UV- Visible, FT - IR).

Irradiation technique

A local made irradiation device containing an 18-watt ultraviolet lamp with a length of 589 mm and a diameter of 26 mm, a 365 nm light intensity with a radiation range of 270-400 nm was used. The polymer films were placed in the device parallel to the lamp and fixed from the source for all samples to ensure that the radiation of all polymers reached the same intensity and amount. The duration of irradiation for different periods of time was as follows 10, 20, 40, 80, 120, and 160 hours

respectively, and after each irradiation the optical degradation of polymer films was monitored using spectral measurements of FT-IR, UV-Visible, and microscopic examination.

Spectral study for MgO NPS

The morphological properties and crystalline properties of the sample were studied through x-ray diffraction (XRD), surface morphology analysis by SEM microscopy and AFM.

Observation of the optical degradation of PMMA films UV-Visible spectroscopy

The value of the constants of photo-degradation (Kd) of the absorbance values was calculated on the basis of the data indicated by UV spectra within the range (200- 700) nm after the irradiation process and at different time intervals by the following equation:

$$\ln(A_{\infty} - A_t) = \ln(A_{\infty} - A_0) - K_d t \dots \dots 1$$

Where, (A_0) the absorbance of polymer film before irradiation, (A_t) absorption at irradiation time (t) for the same film, and (A_{∞}) the absorption of polymeric films at infinity of time.

The photo-degradation constant of polymer films (-Kd) was derived from the slope of the plot of relationship between $\ln(A_{\infty} - A_0)$ with the irradiation time, and finding the linear line slope which represent (-Kd).

Fourier transform infrared spectroscopy

To calculate the growth of the hydroxyl, carbonyl groups, a reference peak was selected at the wave number 1435 cm^{-1} which refers to the (skeletal CH_2 deformation) in PMMA (23) as a guide to comparing its absorption with PMMA absorption using the base line method (24).

$$I_s = \frac{A_s}{A_r} \dots \dots 2 \quad \text{Where,}$$

I_s = Index of the group under study,
 A_s = absorption of the peak under study,
 A_r = absorption of the reference under study.

By using the Beer-Lambert law, absorption (A) was converted to transmutation (T%) (25)

$$A = \log 100/T\% = 2 \log T\% \dots \dots 3$$

The active chemical groups of the model were identified using spectroscopy FTIR, the photolysis of polymeric films was followed by the incident frequency of the index value of the carbonyl coefficient of growth (I_{CO}) and the incident frequency of the index value of the hydroxyl coefficient of growth (I_{OH}) by measuring growth, for the purpose of ultraviolet radiation determination of the intensity of absorbed packets calculated before and after irradiation (23,26).

Results and Discussion:
Structural characterization
XRD measurements

The XRD techniques are used to observe structure of nanoparticles and crystalline properties of particles **Fig.1** shows the X-ray diffraction of MgO NPs synthesized using the precipitation method. The size of MgO NPs was attained by Debye-Scherrer's equation $D = K\lambda/\beta\cos\theta$

Where D is the size of the crystal; K is constant its value (0.9); λ , β are the full width half maximum (FWHM), which indicate and confirm that the MgO NPs has face centered cubic (fcc). That is compatible with the results of the literature (27). X-ray diffraction patterns of the MgO NPs showed in comparison to the standard reference of JCPDS No. (98-000-5910) that the peaks of diffraction (100), (111), (200), (220), (311) and (222) are assigned at angles (34.3°, 37.43°, 62.25°, 74.8°, 78.83°), respectively.

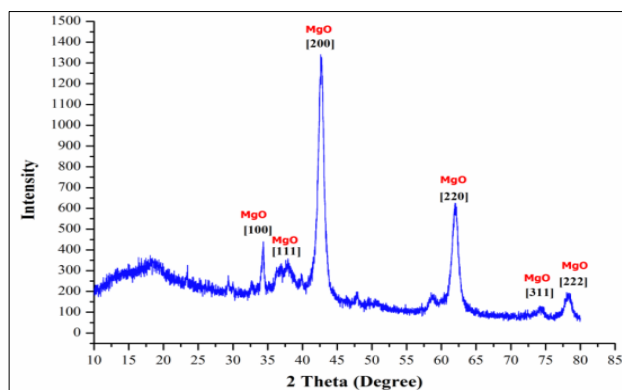


Figure 1. XRD patterns of synthesized MgO nanoparticles using the precipitation method

SEM Measurements

Figs. 2 (A,B,C) present the (SEM) images of the MgO NPs synthesized precipitation method in showed of floral or spherical nano shapes.

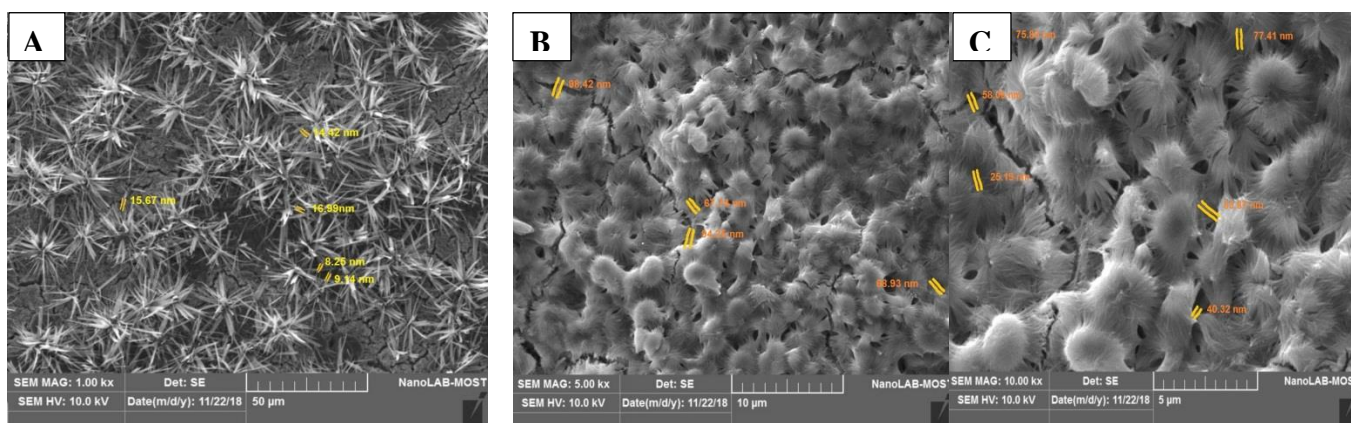


Figure 2 . (A,B,C) SEM images of the MgO NPs synthesized precipitation method with the different shapes

AFM Measurements

AFM results gave two-dimensional and three-dimensional images of the surface of the MgO NPS by precipitation method as shown in Figs. 3

and 4 which demonstrate the average distribution of the prepared nanoparticles, where the average grain size was 57.03 nm.

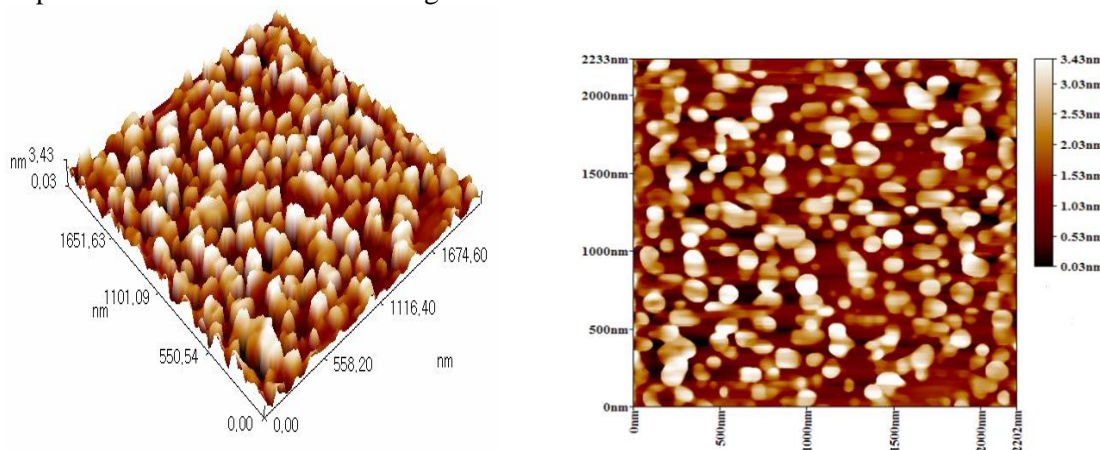


Figure 3. AFM image of 2-dimensional and 3-dimensional of MgO NPS

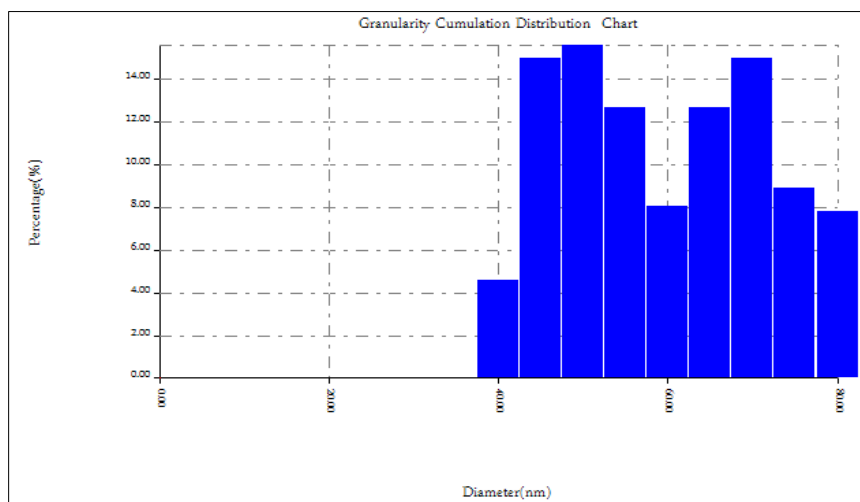


Figure 4. The average distribution for MgO NPS

UV-Visible spectroscopy of PMMA films

The optical properties of MgO NPs were characterized by spectroscopy of UV rays. The spectra of the samples were recorded within the range of wavelength lengths (200 - 700) nm, at 25°C (18). During the various irradiation periods that were exposed to the thin slices of polymer, by spectrophotometer (UV-Visible, Jenway, Model 6800) it was observed that the polymer film began to undergo a simple crush after increasing irradiation periods of 120 hours and a clear increase after 160 hours. Tab.1 gives information on the extent of the increase in photolysis of the polymer

slices. The value of the constant (K_d) calculated in Tab.2 is based on the data indicated by UV spectra after the irradiation process and at different times (was calculated according to Eq.1). The change in the absorption spectra of polymer films prepared with a thickness of $(70 \pm 5) \mu\text{m}$ and the container at different concentrations at the different times of irradiation is due to the increase of the light-absorbing functional groups (28,29). The highest absorption value at time is 160 hours as in Figs. 5-7. Tab.2 indicates that the MgO increases the speed of light interaction with the polymer and that the reaction is first order (30), as in Figs.8,9.

Table 1. Absorbance of the PMMA with thickness $70 \pm 5 \mu\text{m}$ with the different concentrations of the MgO NPS and calculated at 270 nm spectrum measurements of UV-Vis with time

Irradiation Time (hrs.)	Absorbance					
	0	20	40	80	120	160
PMMA	0.098	0.150	0.191	0.258	0.360	0.542
PMMA + 0.025 % MgO	0.114	0.258	0.353	0.540	0.648	0.779
PMMA + 0.05% MgO	0.117	0.339	0.457	0.602	0.707	0.900
PMMA + 0.1 % MgO	0.122	0.406	0.541	0.722	0.812	0.958
PMMA + 0.2 % MgO	0.124	0.469	0.598	0.779	0.957	1.082
PMMA + 0.4% MgO	0.130	0.539	0.757	0.901	1.129	1.262

Table 2. Values constants of rate decomposition K_d of the MgO NPS in PMMA films

Concentrations %	K_d (Sec.) ⁻¹ x 10 ⁻⁵
0.025	0.218
0.05	0.222
0.1	0.235
0.2	0.257
0.4	0.278

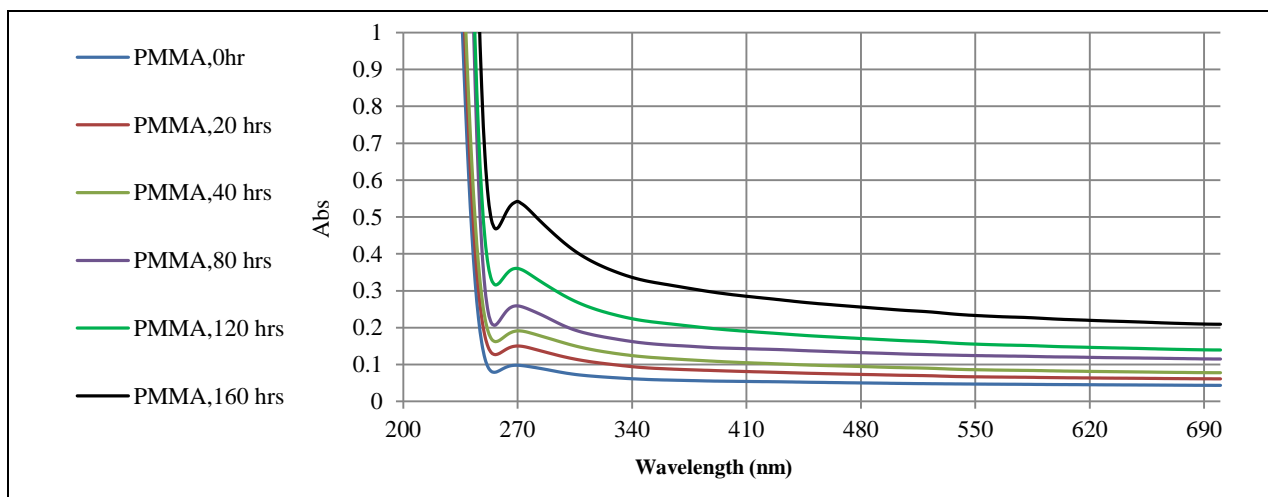


Figure 5. Change in the spectrum of UV-Vis for pure PMMA with thickness $70 \pm 5 \mu\text{m}$ at different times of irradiation

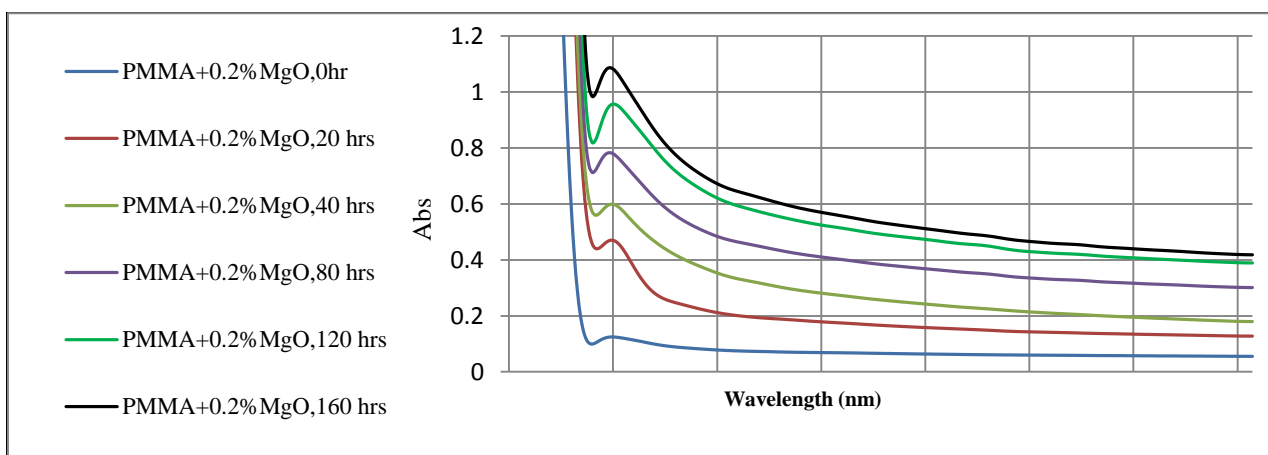


Figure 6. Change in the spectrum of UV-Vis for PMMA containing (0.2%) of the MgO NPS with thickness $70 \pm 5 \mu\text{m}$ at different times of irradiation

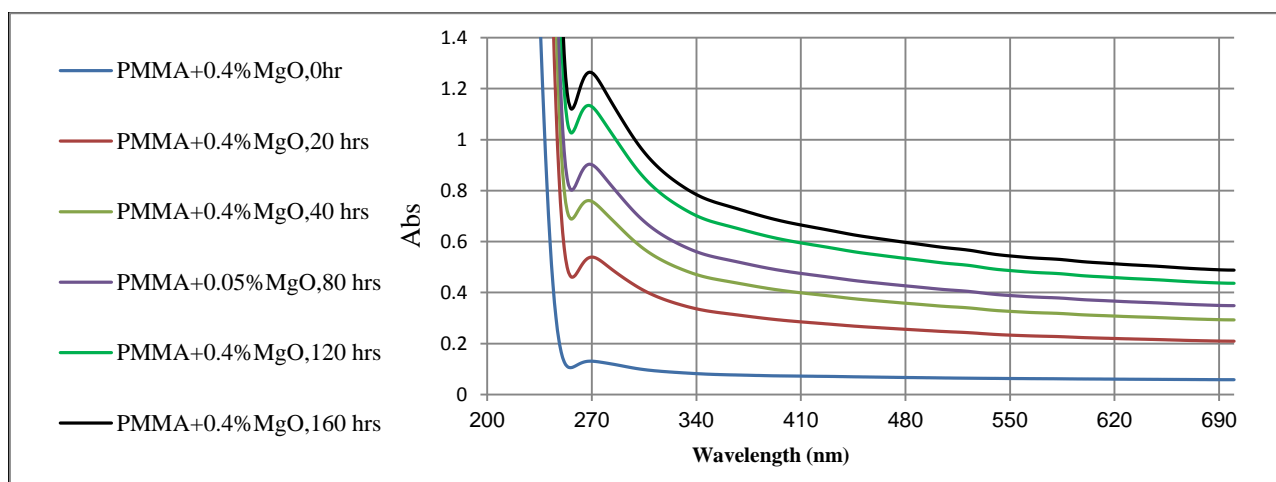


Figure 7. Change in the spectrum of UV-Vis for PMMA containing (0.4%) of the MgO NPS with thickness $70 \pm 5 \mu\text{m}$ at different times of irradiation

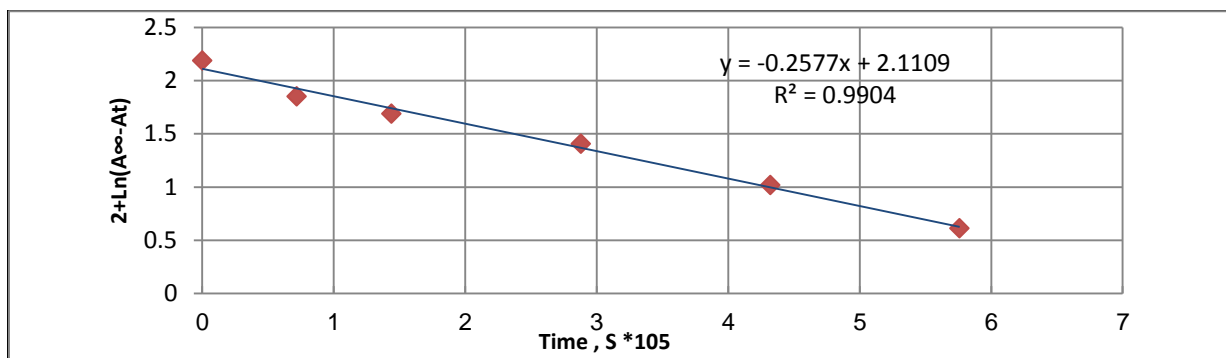


Figure 8. The relationship between the logarithm of PMMA films containing of (MgO NPS) with thickness $70\pm 5 \mu\text{m}$ and (0.2%) with irradiation time

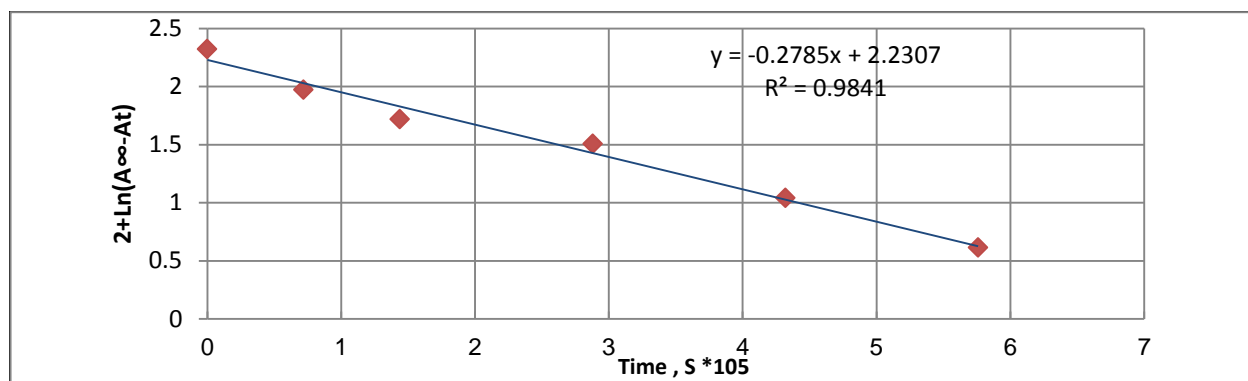


Figure 9. The relationship between the logarithm of PMMA films containing of (MgO NPS) with thickness $70\pm 5 \mu\text{m}$ and (0.4%) with irradiation time

FT-IR spectroscopy of PMMA films

Photolysis of the polymer films slices was monitored using (FT-IR, ATR, Tensor 27, Bruker, Germany) spectrometer. The absorption spectrum of the polymer films gave range between $(400-4000) \text{ cm}^{-1}$. The frequency of the carbonyl (C=O) at the $(1725) \text{ cm}^{-1}$ (31), Hydroxyl(OH) was at region

$(3200-3600) \text{ cm}^{-1}$ position (32). The photo-degradation throughout different irradiation times was followed by notation changes in the carbonyl, and hydroxyl absorption peaks. The FT-IR spectra of PMMA pure films and the films of PMMA containing MgO nanoparticles before and after irradiation (160 h) are shown in Figs.10, 11, 12.

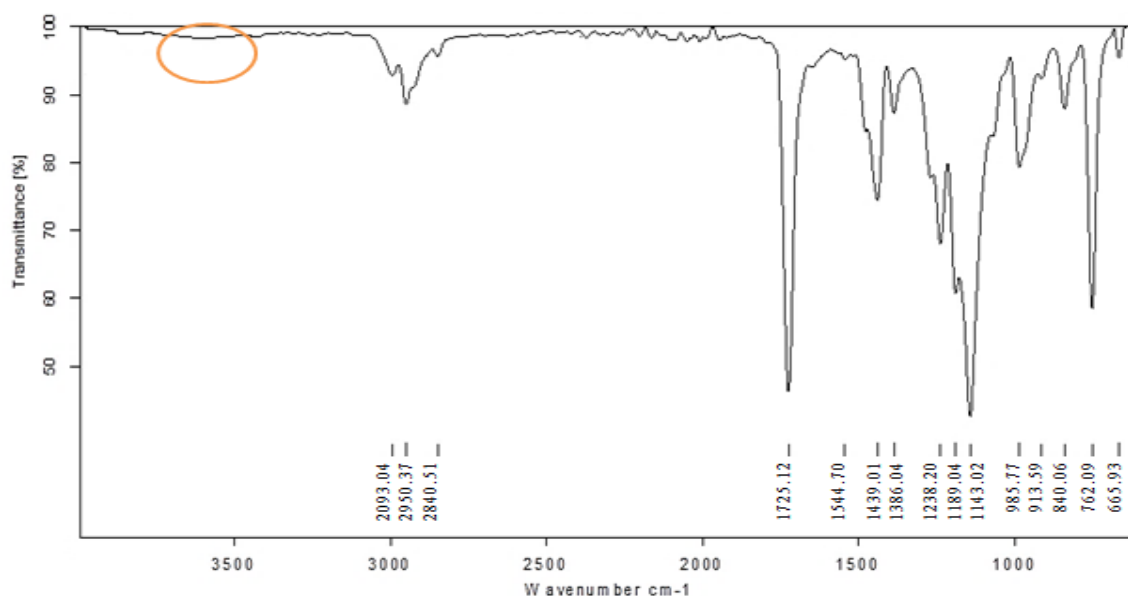


Figure 10. FT-IR spectrum of PMMA pure film with thickness $70\pm 5 \mu\text{m}$ before irradiation time

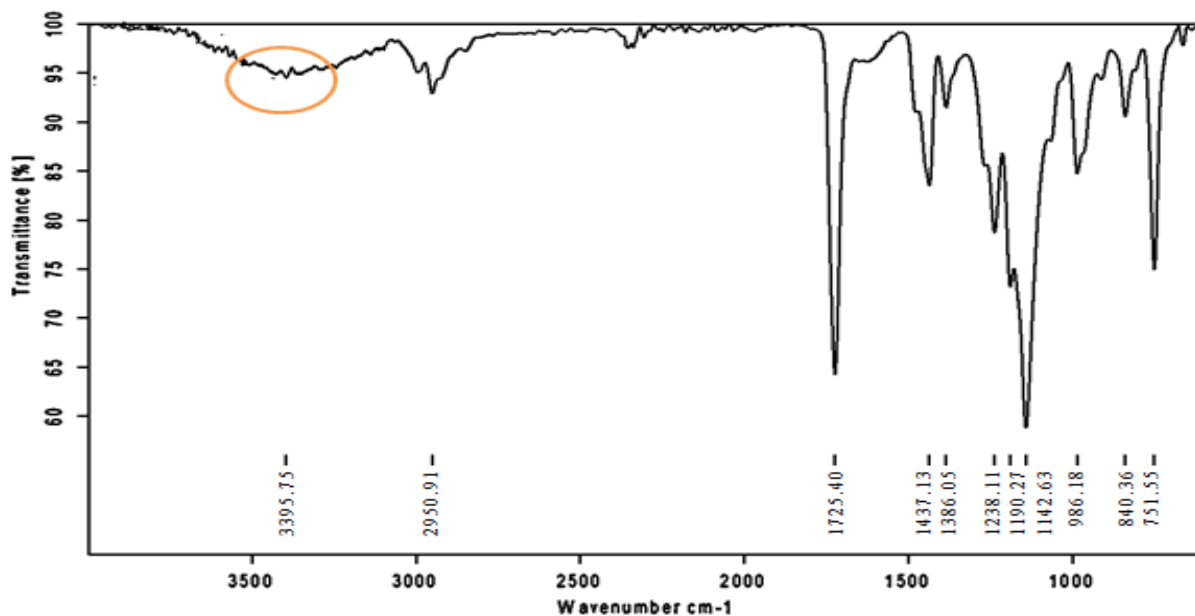


Figure 11. FT-IR spectrum of PMMA film with thickness $70\pm 5 \mu\text{m}$ containing concentration (0.4 %) of the MgO NPS before irradiation time

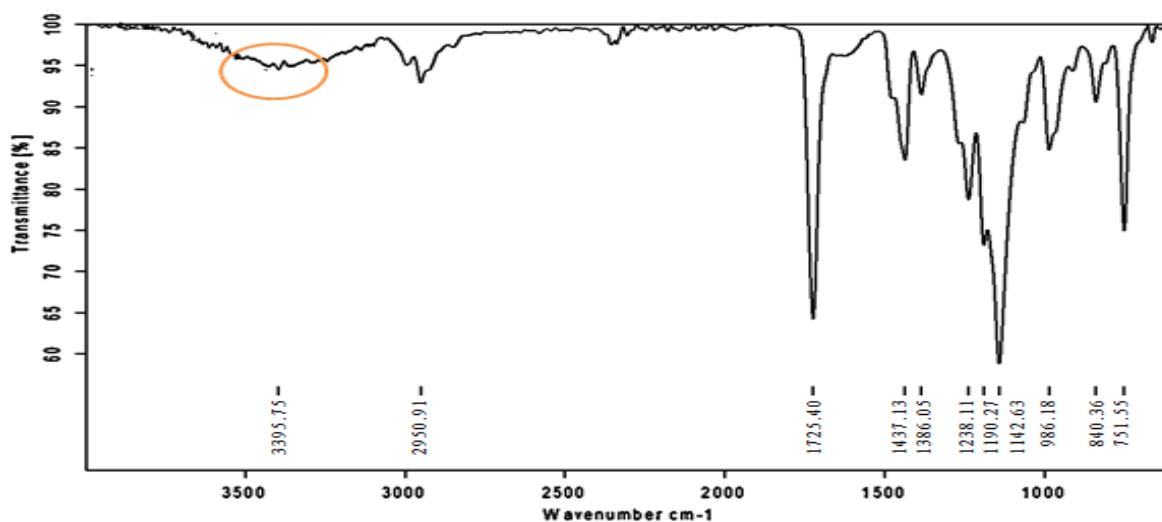


Figure 12. FT-IR spectrum of PMMA film with thickness $70\pm 5 \mu\text{m}$ containing concentration (0.4%) of the MgO NPS and the time of irradiation 160 hrs.

When comparing the FT-IR spectra of pure PMMA film with the film containing 0.4% concentration of MgO NPS after irradiation for 160 hours, it has been noted that the peak of the PMMA films containing MgO nanoparticles absorbing was higher than the pure film absorption film. It means that the magnesium oxide hastens photo-degradation. This is similar to previous studies involving the addition of materials to the polymer (33).

The values of the (I_{OH}) absorption coefficient for the pure PMMA film as well as the films containing different concentrations of MgO NPS were calculated as in Tab.3 The values of the hydroxyl group (I_{OH}) absorption coefficient of pure films of PMMA were increased with increasing time of irradiation and that the hydroxyl group absorption coefficient is 0.00 before the irradiation process and at the highest 160 hour time of 0.301 for the same conditions. This corresponds to the other times of the irradiation for polymeric films.

Table 3. Coefficient growth values hydroxyl (I_{OH}) with irradiation time for PMMA containing concentrations different of the (MgO NPS)

Irradiation time (hrs.) Wt. % of Addition	Hydroxyl Index (I_{OH})				
	0.0	40	80	120	160
PMMA	0.00	0.055	0.157	0.257	0.301
PMMA + 0.025 % MgO	0.000	0.095	0.226	0.309	0.364
PMMA + 0.05% MgO	0.000	0.126	0.338	0.346	0.410
PMMA + 0.1 % MgO	0.000	0.178	0.344	0.370	0.453
PMMA + 0.2 % MgO	0.000	0.234	0.357	0.412	0.484
PMMA + 0.4% MgO	0.000	0.288	0.396	0.451	0.501

The increase with the increased absorption of polymeric films to UV radiation during the irradiation process and the values of the coefficient of absorption of the hydroxyl group (I_{OH}) increased the speed of disintegration of optical oxidation of polymer films(34).

Optical microscope

Pure PMMA films and polymer films containing concentrated 0.4%. form magnesium oxide nanoparticles showed there is a change and deformation of the film surface with irradiation time.as Figs. 24 and 25. This fits in with the surface morphology.

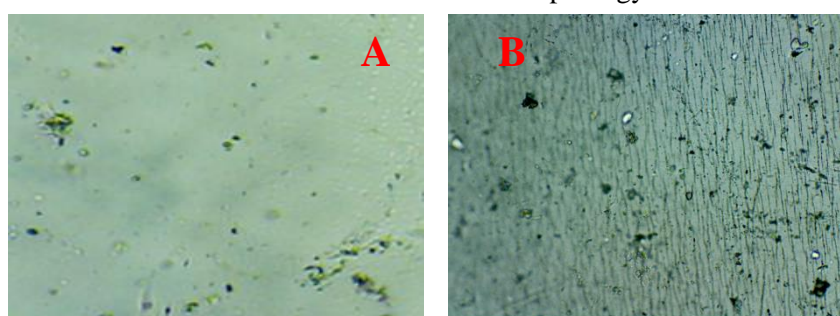


Figure 13. The change in the pure film surface of PMMA: (A) before irradiation time, (B) at 120 hours

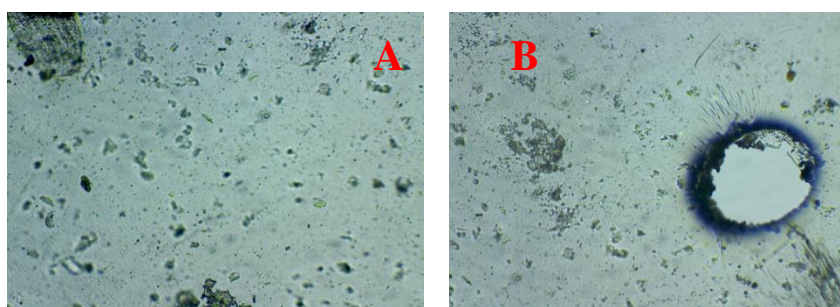


Figure 14. The change in the film surface films of PMMA containing concentrations 0.4% of the MgO NPS at 120 hours

Conclusions:

The use of magnesium oxide nanoparticles prepared as catalysts help to boost the photo-degradation of PMMA films after irradiation with ultraviolet light for distinct periods. Several occurring sequential processes make the molecular mass lower. Other chemical reactions result in breakage in weak bonds, Cross-linking, as well as secondary oxidative reactions, and Chain – scission. Several techniques are used to monitor photo-degradation such as growth of specific functional groups in the infrared spectrum, chain scission and rate of deterioration in molecular mass, proportion

of mass loss. In addition to this, the atomic force and scanning electron microscopy are used to characterize and assess the surface morphology of magnesium oxide nano particles. The results indicate that the rate of photo-degradation is affected by the chemical structure of polymer and additives. The mixed films show important photo catalytic behavior in contrast to pure films. The existence of additives in polymers films hastens photo-degradation compared to pure films.

Authors' declaration:

- Conflicts of Interest: None.
- We hereby confirm that all the Figures and Tables in the manuscript are mine ours. Besides, the Figures and images, which are not mine ours, have been given the permission for re-publication attached with the manuscript.
- Ethical Clearance: The project was approved by the local ethical committee in University of Al-Anbar.

References:

1. Ul-Islam S, Butola BS. Nanomaterials in the wet processing of textiles. Nano-Zinc Oxide: Prospects in the Textile Industry 1st ed. John Wiley & Sons. 2018, Chap 3; p.113-134.
2. Singh, N, Khanna P K. In situ synthesis of silver nanoparticles in poly (methyl methacrylate). Mater Chem Phys. 2007; 104 (2-3): 367-372.
3. Król A, Pomastowski P, Rafińska K, Railean PV, Buszewski B. Zinc oxide nanoparticles: Synthesis, antiseptic activity and toxicity mechanism. Adv Colloid Interface Sci. 2017; 249: 37-52.
4. Hanaa S M. Effect of gamma irradiation and ZnO nano particles on the A.C electrical conductivity of polyaniline. IJP. 2017; 15 (32):130-135.
5. Paula A , Humberto P, Boris D, Andrea A, Francesca S, Maria P , et al. Effect of CaCO₃ nanoparticles on the mechanical and photo-degradation properties of LDPE. Molecules. 2018; 24 (1): 1-12.
6. Çaykara T, Güven O. UV degradation of poly (methyl methacrylate) and its vinyl tri ethoxysilane containing copolymers. Polym. Degrad. Stab 1999; 65 (2): 225-229.
7. Bdaiwi W. Reinforcement of poly (methyl methacrylate) by ZrO₂Y₂O₃ nanoparticles used in medical applications. J Optoelectron Adv M. 2018; 10 (1): 1-10.
8. Shanti R, Hadi A, Salim Y, Ramesh S, Ramesh K. Degradation of ultra-high molecular weight poly (methyl methacrylate-co-butyl acrylate-co-acrylic acid) under ultra violet irradiation . Rsc Adv. 2017; 7(1):112-120.
9. Susheel K, editor. Biodegradable green composites. Wiley & Sons. 2016. 368 P
10. Kumar V, Sonkawade R, Ali Y, Dhaliwal A. Study of chemical, optical and structural properties of 120 MeV Ni 11 ions beam irradiated poly (ethylene terephthalate) film. Int. J Appl Eng Res.. 2011; 2 (2): 419-430.
11. Abdus M, Pallab C, Prosenjit S. Synthesis, structure, spectroscopy and photocatalytic studies of nano multi-metal oxide MgO·Al₂O₃·ZnO and MgO·Al₂O₃·ZnO·curcumin composite. Int J Nanosci Nanotechnol. 2017; 13(1): 69-82.
12. Subhan M, Tanzir A, Hiroyasu N, Mika S, Moon K. Synthesis, structure, luminescence and photophysical properties of nano CuO· ZnO· ZnAl₂O₄ multi metal oxide. J Lumin. 2014; 148 (98): 123-127.
13. Wang L, Wang J, den E, Wu J, Jia X. Controlled synthesis of magnesium oxide nanoparticles for dye adsorption. J Nanoelectron Optoe. 2017; 12 (5): 512-517.
14. Yang Q, Sha J, Wang L, Wang J, Yang D. MgO nanostructures synthesized by thermal evaporation. Mater Sci Eng. 2006; 26 (5-7): 1097-1101.
15. Ouraipryvan P, Sreethawong T, Chavadej S. Synthesis of crystalline MgO nanoparticle with mesoporous-assembled structure via a surfactant-modified sol-gel process. Mater Lett. 2009; 63(21): 1862-1865.
16. Hao Y, Meng G, Ye C, Zhang X, Zhang L. Kinetics-driven growth of orthogonally branched single-crystalline magnesium oxide nanostructures. J Phys Chem B . 2005; 109 (22): 11204-11208.
17. Yi X, Wenzhong W, Yitai Q, Li Y, Zhiwen C. Deposition and microstructural characterization of MgO thin films by a spray pyrolysis method. Surf Coat Technol. 1996; 82 (3): 291-293.
18. Kumari L, Li W Z, Vannoy C H, Leblanc R M, Wang D Z. Synthesis characterization and optical properties of Mg(OH)₂ micro-/nanostructure and its conversion to MgO. Ceram Int. 2009; 35 (8): 3355-3364.
19. Yanan Z, Yue Z, Haoshuang G. Ultraviolet detectors based on wide bandgap semiconductor nanowire: A review. Sensors. 2018; 18 (7): 2072-2080.
20. Kaczmarek H, Kaminski A, Herk A. Photo oxidative degradation of poly (alkyl methacrylate)s . Eur Polym J. 2000; 36 (4): 767-777.
21. Karthikeyan K, Poornaprakash N, Selvakumar N, Jeyasubramanian K. Thermal properties and morphology of MgO-PVA nanocomposite film. J Nanostruct Polym. Nanocomposites. 2009; 5 (4): 83-88.
22. Park J, Lee Y, Yim D. Chemical synthesis and characterization of highly oil Dispersed MgO Nanoparticles. J Ind Eng Chem. 2006; 12 (6): 882-887.
23. Hamed K. Studying the effect of adding pulverized egg shell on the photo-physical properties of polyvinyl alcohol. JESCS. 2019; 14 (4): 2413-2423. (In Arabic)
24. Sibokoza S B, Moloto M J, Mtunzi F, Moloto N. Di phenyl diselenide mediated synthesis of copper selenide nanoparticles and their poly (methyl methacrylate) nanofibers. Asian J. Chem. 2018; 30 (7): 1455-1459.
25. Saeed RK, Mobin T, Vilayat A, Patrick F, Mansoor A. Stability characterization, kinetics and mechanism of degradation of dantrolene in aqueous solution: Effect of pH and temperature. Pharmacol Pharm . 2012; 3 (3): 281-290.
26. Kuzina I, Mikhailov A. The photo-oxidation of polymers in the main reaction of chain propagation in polystyrene photo-oxidation. Eur. Polym. J. 1998; 34(8): 1157-1162.
27. Aseel M, Itab F, Ahmed F. Producing high purity of metal oxide nano structural using simple chemical method. J Phys Conf. 2018; 1032: 12036-12044.
28. Di Mauro A, Cantarella M, Nicotra G, Privitera V, Impellizzeri G. Low temperature atomic layer

- deposition of ZnO: applications in photocatalysis. Appl Catal B . 2016; 196: 68–76.
29. Di A, Cantarella M, Nicotra G, Pellegrino G, Gulino A. Novel synthesis of ZnO/PMMA nanocomposites for photocatalytic applications. Sci Rep. 2017; 7 (1): 334-345.
30. Abdul M, Hussein IF, Abd RO. Fabrication of high responsively for MgO NPs/PSi heterojunction device by sol-gel technique. Silicon. 2019; 9 (5): 311-323.
31. Adil A, Emad A. Study the rate constant of photo decomposition of polystyrene films in presence of some 4- amino-5-(2-(6-methoxynaphthalen-2-yl) piperidino)-1,2,4-triazole-3-thion complexes. ANJS. 2016; 19 (1): 69-75.
32. Anju V, Narayanankutty S. Impact of bis-(3-triethoxysilylpropyl) tetra sulphid on the properties of PMMA/cellulose composite. Polym. 2017; 119: 224–237.
33. Lee Y, Viswanath D. Degradation of poly (methyl methacrylate) (PMMA) with aluminum nitride and alumina. Polym Eng Sci. 2000; 40 (11): 2332-2341.
34. Hamad D, Mehrvar M, Dhib R. Kinetic Modeling of Photodegradation of Water-Soluble Polymers in Batch Photochemical Reactor. Kinetic Modeling for Environmental Systems. Intech Open. 2019; 21 (2): 422-431.

دراسة تأثير الجسيمات النانوية لأوكسيد المغنيسيوم المحضر على سطح متعدد المثيل ميثا اكريليت

حميد خالد الدليمي¹

أحمد مشعل محمد²

مصطفى فرج عبد الراوي¹

¹ قسم الكيمياء، كلية التربية للعلوم الصرفة، جامعة الانبار، الرمادي، العراق

² قسم الكيمياء، كلية العلوم، جامعة الانبار، الرمادي، العراق

الخلاصة :

تضمن البحث تحضير أوكسيد المغنيسيوم النانوي (MgO NPS) وتشخيصه ودراسة تأثيره على سطح البوليمر ، باستخدام تراكيز مختلفة من MgO NPS . النتائج تبين بأن اضافة الاوكسيد تزيد من تحلل متعدد المثيل ميثا اكريليت . تم استخدام تقنية الأشعة السينية والمجهر الالكتروني الماسح ومجهر القوة الذرية لدراسة مورفولوجيا السطح وحجم المادة النانوية. حضرت الرقائق البوليمرية بخلط نسب وزنية مختلفة من اوكسيد المغنيسيوم النانوي بنسبة (0.025 ، 0.05 ، 0.1 ، 0.2 ، 0.4) % مع محلول البوليمر (7% W/V) ، وتم تشيع الرقائق النقية من متعدد المثيل ميثا اكريليت والحاوية على تراكيز مختلفة من أوكسيد المغنيسيوم النانوي باستعمال جهاز الأشعة فوق البنفسجية ، وتم متابعة التغير بثابت سرعة التحلل الضوئي (K_d) باستعمال مطيافية الأشعة فوق البنفسجية ، كما تم متابعة وحساب التغير في مقدار معامل نمو الهيدروكسيل (I_{OH}) باستعمال مطيافية الأشعة تحت الحمراء . بينت النتائج التي تم التوصل إليها أن ثابت سرعة التحلل الضوئي ومعامل نمو الهيدروكسيل تزداد بازدياد فترات التشيع وزيادة تركيز المادة النانوية في الرقائق البوليمرية .

الكلمات المفتاحية: أوكسيد المغنيسيوم، التحلل الضوئي، متعدد مثيل ميثا اكريليت ، MgO NPS ، جسيمات نانوية .